Rare Metal Materials and Engineering
Volume 54, Issue 10, October 2025
Available online at www.rmme.ac.cn

Science Press

Cite this article as: Zhi Hui, Hou Jinxiong, Ma Shengguo, et al. Size Effect of Flow Stress in CoCrNi Medium Entropy Alloy Ultrathin Strips[J]. Rare Metal Materials and Engineering, 2025, 54(10): 2494-2500. DOI: https://doi.org/10.12442/j.issn.1002-185X.20240515.

ARTICLE

Size Effect of Flow Stress in CoCrNi Medium Entropy Alloy Ultrathin Strips

Zhi Hui[1,2,3,4], Hou Jinxiong[1,2], Ma Shengguo[1,3], Wang Tao[1,2], Wang Zhihua[1,3], Huang Qingxue[1,2]

[1] College of Mechanical Engineering, Taiyuan University of Technology, Taiyuan 030024, China; [2] Engineering Research Center of Advanced Metal Composites Forming Technology and Equipment, Ministry of Education, Taiyuan University of Technology, Taiyuan 030024, China; [3] Institute of Applied Mechanics, College of Aeronautics and Astronautics, Taiyuan University of Technology, Taiyuan 030024, China; [4] Department of Mechanics, Jinzhong University, Jinzhong 030619, China

Abstract: A constitutive model considering the size effect was established to investigate the behavior of CoCrNi medium entropy alloy ultrathin strip in different deformation stages during the uniaxial quasi-static tensile test. Results show that when the *t*/*d* value is lower than 10.62, the CoCrNi alloy ultrathin strip shows an obvious size-dependent property in the elastic deformation stage. With the decrease in *t*/*d* value, the volume fraction of the surface layer grains is increased, leading to the linear decrease in flow stress. In the plastic deformation stage, the material stiffness is correlated with the *t*/*d* value. Specifically, as the *t*/*d* value increases, the work-hardening capacity of the material is enhanced. When the *t*/*d* value increases to 10, the work-hardening capacity reaches a maximum state; when the *t*/*d* value is beyond 10, the work-hardening capacity weakens.

Key words: medium-entropy alloy; ultrathin strip; size effect; flow stress; plastic stiffness

1 Introduction

The mechanical properties, such as strength and flexibility, of some thin metal strips show different change laws compared with those of the conventional materials during the deformation process, which is attributed to the size effect[1–6]. For instance, Wang et al[7] examined the deformation behavior of pure tantalum strips with various thicknesses and reported that the tensile strength and yield strength of tantalum strip were increased and the elongation was decreased with the decrease in thickness from 200 μm to 30 μm. This feature reveals that the smaller the thickness, the higher the strength. Sahu et al[8] investigated the mechanical properties and microstructure evolution of SS304 strips and found that both the strength and ductility tend to be inversely related to the size effect, i. e., the thinner the strip, the weaker the mechanical properties. Yuan et al[9] explored the influence of different thicknesses on the mechanical properties of ultrathin aluminum strips by combining experimental results and numerical simulations. It was found that the tensile strength gradually decreased when the sample thickness reduced from 276 μm to 21 μm, and the failure mechanism of the sample changed from brittle to ductile failure. The thickness possesses a substantial influence on the mechanical properties of ultrathin aluminum strips. Additionally, numerous researches have revealed that the ratio of sample thickness to grain size (*t*/*d*) can be taken as a crucial size parameter. Gau et al[2] found that the strength change law was closely related to *t*/*d* through the tensile and three-point bending tests of industrial-pure aluminum strips. However, the traditional theory cannot be applied to ultrathin materials, such as industrial-pure titanium strips[10–11], low carbon steel strips[12],

Received date: October 13, 2024
Foundation item: National Natural Science Foundation of China (12072220, 12225207, 12372364); National Key Research and Development Program (2018YFA0707300); Major Program of National Natural Science Foundation of China (U22A20188); Central Guidance on Local Science and Technology Development Fund of Shanxi Province (YDZJSX2021B002); Natural Science Foundation of Shanxi Province (202303021211038)
Corresponding author: Wang Tao, Ph. D., Professor, College of Mechanical Engineering, Taiyuan University of Technology, Taiyuan 030024, P. R. China, E-mail: twang@tyut.edu.cn; Hou Jinxiong, Ph. D., Associate Professor, College of Mechanical Engineering, Taiyuan University of Technology, Taiyuan 030024, P. R. China, Tel: 0086-351-6111588, E-mail: jxhou@tyut.edu.cn

industrial-pure copper strips[13–14], and CuZn36 strips[6]. In addition, during the micro-forming processes, such as ultrathin strip rolling, the grain size, sample thickness, and texture evolution also exert an influence on dislocation motion, thereby leading to a unique size effect on the strength and ductility of ultrathin materials[15–16].

Recently, CoCrNi medium entropy alloy (MEA) has attracted much attention due to its excellent comprehensive properties, including superconducting and soft magnetic properties, thermal stability[17–18], corrosion resistance, oxidation resistance, resistance to radiation and hydrogen embrittlement, welding formability, and other physical and chemical properties[19–22]. Particularly, CoCrNi MEA has excellent tensile plasticity, which results from its face-centered cubic structure[23]. Therefore, MEA is expected to be employed in cold-forming processing and manufacturing for precision instruments and other fields.

In this research, considering the size effect in the preparation of CoCrNi MEA ultrathin strips, the deformation behavior of CoCrNi MEA with different thicknesses after recrystallization was examined, and a modified constitutive model was established to explain the size effect on the mechanical behavior of ultrathin CoCrNi MEA strips.

2 Experiment

In this research, Co, Cr, and Ni materials (purity>99.9%) with equal atomic ratios were employed as raw materials to form CoCrNi MEA, and the MEA ingot was melted at least 5 times in a vacuum magnetic levitation melting furnace for homogenous composition. To ensure the chemical uniformity of the alloy, the whole process was conducted under argon atmosphere protection, and the homogenization temperature was 1100 °C. After homogenization for 5 h, the ingot was water quenched. Finally, ultrathin CoCrNi MEA strips with different thicknesses were obtained by a twin-roll synchronous rolling mill.

Subsequently, recrystallization was performed on the CoCrNi strip. The annealing temperature was 1050 °C and the annealing time was 30 min. After annealing, the strips were cooled in furnace. Then, the obtained ultrathin strips were subjected to quasi-static tensile tests at room temperature with a strain rate of 2×10^{-4} s^{-1}. The tensile test samples were cut by the electric discharge machining with the support of the sheet plate. Tensile tests were performed on an INSTRON 5969 electronic universal testing machine, and the sample dimensions were 60.0 mm (length)×25.0 mm (width)×6 mm (thickness). All tests were repeated at least three times. An optical microscope (JEOL-JSM-IT500) and an electron emission gun scanning electron microscope (SEM) equipped with an electron backscatter diffractometer (EBSD) were employed for detection. Accelerator voltage, sample inclination angle, and working distance were set as 50 kV, 70°, and 15 mm, respectively. EBSD data analysis was performed using HKL Channel 5 software.

3 Results

Fig. 1a shows the true stress-true strain curves of CoCrNi MEA strips with different thicknesses, where various *t*/*d* values can be obtained since the strips were subjected to annealing treatment at 1050 °C for 30 min. The detailed tensile test results are listed in Table 1, where the yield strength (YS), ultimate tensile strength (UTS), and elongation

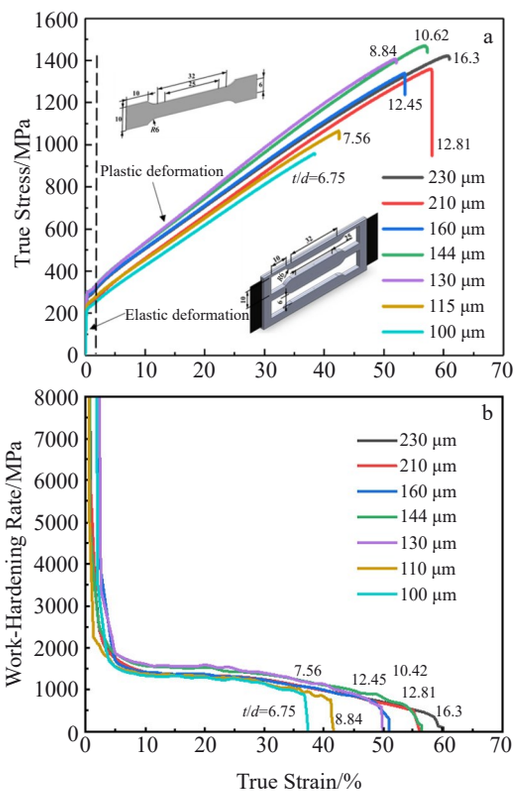

Fig.1 True stress-true strain curves (a) and work-hardening rate curves (b) of CoCrNi MEA strips of different thicknesses

Table 1 Experiment results of tensile tests

No.	Thickness/μm	Grain diameter/μm	*t*/*d*	YS, σ_s/MPa	UTS, σ_b/MPa	Elongation, ε/%
1	100	14.81	6.75	222.14	958.06	38.36
2	115	15.21	7.56	244.63	1065.65	42.42
3	130	14.71	8.84	300.19	1406.70	51.91
4	144	13.56	10.62	302.33	1469.13	56.76
5	160	12.85	12.45	286.32	1338.43	53.40
6	210	16.39	12.81	278.51	1359.19	57.90
7	230	14.11	16.30	279.18	1420.98	60.39

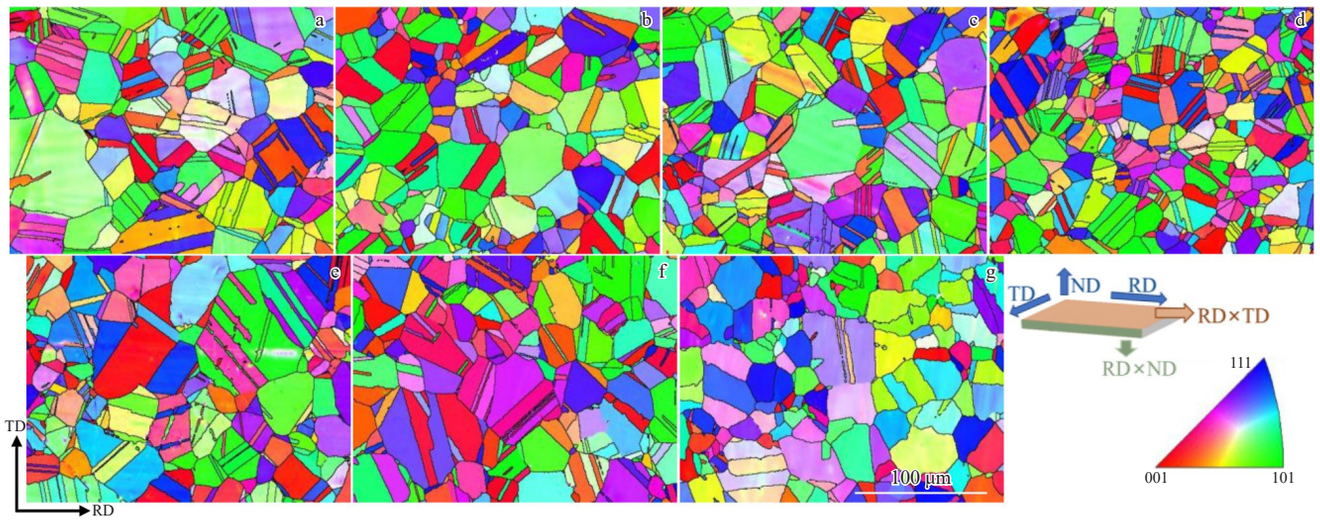

Fig.2 IPFs of CoCrNi MEA strips of thickness of 100 μm (a), 115 μm (b), 130 μm (c), 144 μm (d), 160 μm (e), 210 μm (f), and 230 μm (g)

are indexed as σ_s, σ_b, and ε, respectively. Fig. 2 illustrates the inverse pole figures (IPFs) of CoCrNi MEA strips of different thicknesses. TD, RD, and ND represent the transverse direction, rolling direction, and normal direction, respectively. The average grain diameter can be obtained according to Fig.2. It is worth mentioning that the average grain size has no obvious dependency on the sample thickness. YS and UTS substantially rise with the increase in thickness, whereas the average grain size does not show any significant changes. With the decrease in thickness, the *t*/*d* value is gradually reduced, and YS and UTS are firstly increased and then decreased. As the *t*/*d* value reduces from 10.62 to 6.75, YS and UTS exhibit a reducing trend. However, when the *t*/*d* value exceeds 10, both the YS and UTS exhibit an obvious growth trend with the decrease in grain size[24].

Fig. 1b shows the work-hardening rate curves of CoCrNi MEA strips of different thicknesses, which exhibit a typical three-stage work-hardening behavior (sharp drop, slight decrease, and continuous decline). The first stage is related to the elastic-to-plastic transition during tensile deformation. In the second stage, which is the relatively stable deformation process, the average value of work-hardening rate of the approximately horizontal curve corresponds to the slope of the elastic deformation stage in Fig. 1a. Therefore, as the strip thickness decreases, the transitions rapidly change to the third stage, namely the continuous reduction stage. The work-hardening rate reaches the maximum value when the thickness is 130 μm. In the third stage, deformation instability occurs and eventually leads to premature fracture.

Fig. 3a shows the relationships between strength and *t*/*d* value of CoCrNi MEA strips. It can be seen that when the *t*/*d* value is lower than 10, both the YS and UTS curves present a linear relationship with *t*/*d*. As the sample tends to be miniaturized, the flow stress variation is significantly affected by the size effect. This phenomenon can be explained by the surface layer model[25], which divides the sample microstructure into inner grains and outer grains of the free surface. During the deformation process, the inner grains of the sample pile up at the grain boundaries through dislocation movement, leading to an increase in YS and UTS. However, grains on the free surface are relatively less constrained. When the dislocation moves to the free surface, it is easier to slip from the crystal surface, so the flow stress of the sample reduces[12].

Fig. 3b illustrates the relationships between UTS and thickness of CoCrNi MEA, Q195 steel, industrial-pure copper T2,

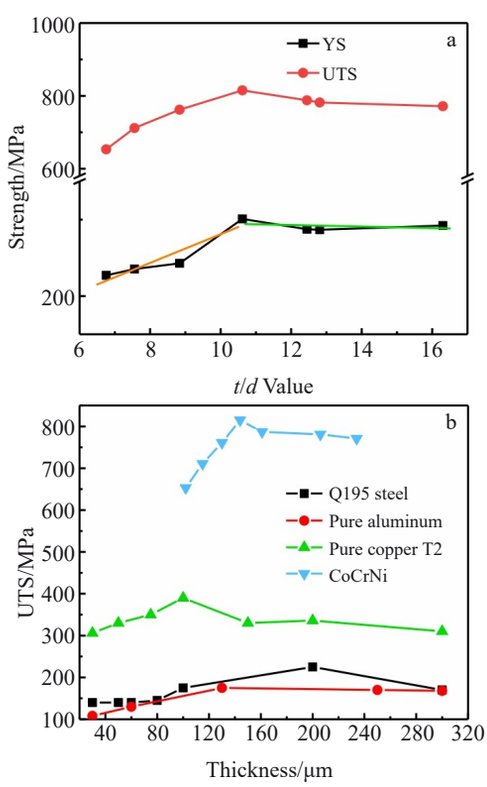

Fig.3 Relationships between strength and *t*/*d* value of CoCrNi MEA strips (a); relationships between UTS and thickness of different alloys[26] (b)

and industrial-pure aluminum[26]. It can be seen that similar size effects occur in the abovementioned materials: UTS is increased and then decreased with the decrease in thickness. More importantly, the CoCrNi MEA strip exhibits much higher strength and a stronger size effect than conventional metallic materials, especially when its thickness is 100–250 μm.

4 Discussion

The true stress-true strain curves can be divided into two stages. One is the elastic deformation stage, and the other is the plastic deformation stage, as shown in Fig. 1a. In each deformation stage, the true stress-true strain curve can be simplified as a linear curve. In this research, the double-line curve is introduced to describe the true stress-true strain curve[27].

4.1 YS predictive model based on Hall-Petch relationship and surface layer effect

The true stress-true strain curve is divided into the elastic deformation stage and the plastic deformation stage, as denoted by the dotted line in Fig. 1a. It is mentioned that CoCrNi MEA strips have a more pronounced size effect than traditional alloys. Generally, the generalized size includes the sample thickness. The effect of the grain size on the plastic deformation is mainly caused by grain sliding, rotation, and distortion. The effect of grain size on flow stress is expressed by the Hall-Petch formula, as follows:

$$\sigma_s = \sigma_0 + Kd^{-0.5} \tag{1}$$

where σ_0 denotes the stress when the grain size is infinite (i.e., the yield stress of a crystal), K reflects the grain boundary effect on the deformation, and d represents the grain size. However, in this research, as the thickness of the CoCrNi MEA strip decreases, the flow stress gradually decreases. It can be seen from Fig. 3a that there is an apparent relationship between YS and t/d. This is mainly ascribed to the fact that the surface layer grains are more easily deformed than the inner grains. Therefore, the effect of the apparent size (length and thickness) on YS should also be considered. The flow stress-strain equation can be expressed by Eq.(2), as follows:

$$\sigma = f(l, t, d) \tag{2}$$

where l, t, and d represent the length, thickness, and grain size of the sample, respectively. In this research, the length can be rationally ignored due to the ultrathin thickness. As a result, the size-dependent flow stress-strain model can be further simplified as Eq.(3), as follows:

$$\sigma = f(t, d) \tag{3}$$

As demonstrated in Fig. 3b, the grains located on the free surface are more confined than those inside the material. Therefore, the surface grains usually do not have a significant effect on the mechanical properties of materials. But when the volume fraction of grains (α_s) in the surface layer increases by decreasing the number of grains along the thickness direction, the flow stress decreases. In this research, only linear relationships are introduced to describe the size effect on flow stress before the yield point. In the elastic deformation stage, the elastic modulus can be considered as a constant, and the plastic behavior of the material is commonly not affected by the sample thickness. One way to quantify the effect of grain size and thickness on YS is to assume that their contributions have a power-law form[28], as expressed by Eq.(4):

$$\sigma_y = \sigma_0 + Kd^{-m} + h(t/d)^{-n} \tag{4}$$

where h is a coefficient; m and n are material-related constants. This formula consists of two main terms: one is the size-independent term, namely the intrinsic YS (σ_0) and the other is the size-dependent term, $Kd^{-m} + h(t/d)^{-n}$. In this case, the following assumptions are made: the first term is essentially based on the grain boundary (d), and the second term is related to surface grains (t/d). In Eq. (4), σ_0+Kd^{-m} is similar to the classic Hall-Petch formula with m=0.5[29–30]. The classical theory for the exponential form in Eq. (4) is mainly based on the activation of dislocation sources due to the dislocation accumulation or work-hardening caused by the overflow of dislocations at the grain boundaries[31]. Therefore, a modified Hall-Petch model can be constructed based on the relationship between YS and t/d, as follows:

$$\sigma_y = \sigma_0 + Kd^{-0.5} + h(t/d)^{-n} \tag{5}$$

Yu et al[32] investigated the YS of copper films on Kapton rubber and found that YS depends largely on the film thickness and can be suitably fitted by σ_y=116+355$t^{-0.473}$. Venkataraman et al[33] examined the effects of grain size and layer thickness on the mechanical properties of Al layers pre-pared by electrolytic thinning on Si substrates. Although the Hall-Petch analysis was used for the grain size effect (i.e., m=0.5), it was found that n=1 was more appropriate for the thickness effect, and m=1 was more reasonable for the grain size effect. In this research, $\sigma_0+Kd^{-0.5}$ can be rationally taken as a constant. In the case of n=−1, two straight lines can be obtained according to Fig.3a, and the fitting formulas are as follows:

$$\sigma_y = \begin{cases} 93.141 + 18.766t/d & 6.75 < t/d < 10.62 \\ 304.818 - 0.996t/d & 10.62 < t/d < 16.3 \end{cases} \tag{6}$$

Table 1 and Table 2 show YS and K parameter under different t/d values, respectively. Therefore, the unknown values of specific parameters from Eq. (5) are obtained; $\sigma_0 = \frac{1}{n}\sum_{n=1}^{7}\sigma_n = 267.51$ MPa, $K_1 = \frac{1}{4}\sum_{n=1}^{4\text{-}1}K_n = -63.53$, and $K_2 = \frac{1}{4}\sum_{n=4\text{-}2}^{7}K_n = 743.54$.

Therefore, the fitting formulas can be further modified, as follows:

$$\sigma_y = \begin{cases} 267.51 - 63.53d^{-0.5} + 18.766(t/d) & 6.75 < t/d < 10.62 \\ 267.51 + 743.54d^{-0.5} - 0.996(t/d) & 10.62 < t/d < 16.3 \end{cases} \tag{7}$$

For the case of 6.75<t/d<10.62, the t/d value determines YS. For the case of 10.62<t/d<16.3, the K value becomes

Table 2 K parameter under different t/d values

No.	1	2	3	4-1	4-2	5	6	7
t/d	16.30	12.81	12.45	10.62	10.62	8.84	7.56	6.75
K	−63.33	−68.26	−60.44	−62.08	717.38	747.09	759.83	749.85

Note: at point 4, the curve has two fitting results, resulting in two t/d values which are denoted as 4-1 and 4-2; at other points, the curves only have one result

positive, indicating that the size effect gradually weakens. Both K and h can be applied to calculate the coefficients in the Hall-Petch relationship. For the case of t/d <10.62, the size dependency is obvious. Fig.4a illustrates the volume fractions of surface and internal grains under different t/d values. The volume fraction of grains in the surface layer is increased with the decrease in t/d value. As the free surface constraint is small, the flow stress weakens. This is essentially ascribed to the fact that dislocation tangles occur near the triple junctions of grain boundaries, and some dislocations are heterogeneously distributed within the grains on the surface[34].

Based on the Hall-Petch relationship and surface layer model, the relationship between YS and t/d value of CoCrNi MEA strips can be rationally estimated. Furthermore, since the surface layer grains are located on the free surface, the constraints are relatively small. Therefore, when the dislocation moves towards the surface layer grains, it can be removed more easily from the crystal surface, so the flow stress reduces. The size effect on the elongation is shown in Fig. 4b. The schematic diagrams inside Fig. 4b show the surface layer change during tensile test. The elongation is reduced with the decrease in t/d value. This fact reveals that although the grain size changes slightly, the elongation is decreased with the reduction in thickness.

4.2 Uniform constitutive model

Fig. 1a shows the relationship between true stress and true strain, and the true stress-true strain curve at this stage can also be simplified as a line, as follows:

$$\sigma = \sigma_y + E''(\varepsilon - \sigma_y/E) \quad \varepsilon > \sigma_y/E$$
$$E'' = \Gamma(d, t) \tag{8}$$

where σ_y represents the YS, E denotes the size-independent elastic modulus[27], E'' signifies the plastic stiffness, and $\Gamma(d, t)$ is a plastic stiffness function.

The plastic stiffness values of metal plates with different t/d are shown in Table 3. Fig.5 illustrates the relationship between plastic stiffness and t/d value, which denotes the work-hardening capability of the strip material. The plastic stiffness corresponds to the slope of the plastic deformation stage in Fig. 1a. Initially, the plastic stiffness rises with the increase in t/d value, but it eventually decreases. The plastic stiffness reaches its maximum when the t/d value is approximately 10.

Hence, the form of the plastic stiffness function Γ is proposed, as follows:

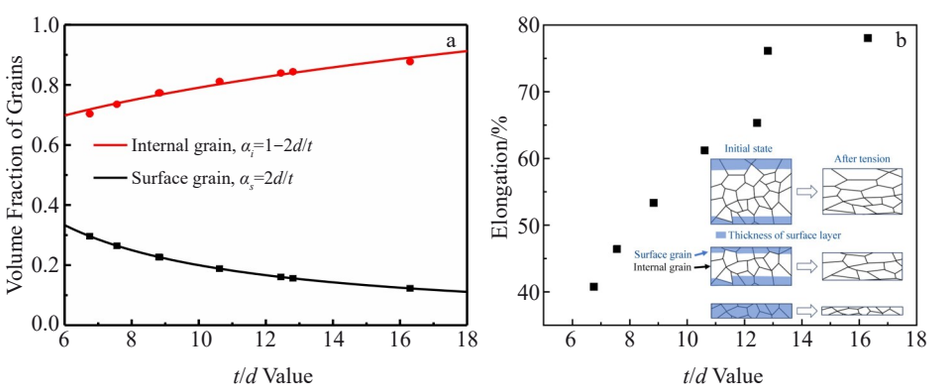

Fig.4 Volume fraction of grains (a) and elongation (b) as a function of t/d value

Table 3 Plastic stiffness under different t/d values (MPa)

t/d	16.30	12.81	12.45	10.62	8.84	7.56	6.75
Plastic stiffness	1942.14	1991.40	1995.64	2154.89	2116.34	1953.41	1928.19

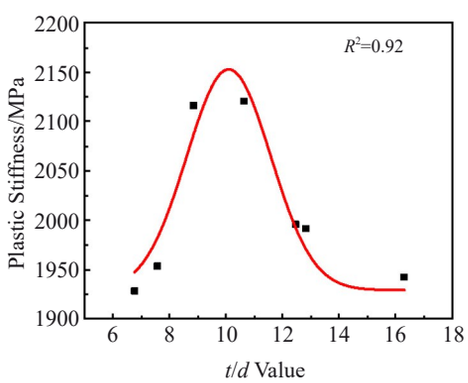

Fig.5 Relationship between plastic stiffness and t/d value

$$\Gamma = p + q\mathrm{e}^{-\frac{(t/d-u)^2}{2v^2}} \tag{9}$$

where p, q, u, and v are parameters corresponding to the plastic stiffness function related to thickness. The parameters p, q, u, and v are 1929.06, 223.90, 10.08, and 1.49, respectively.

Based on the above analysis, a uniform constitutive model considering the effect of grain size and thickness of strip metal can be proposed, as follows:

$$\sigma = \begin{cases} E\varepsilon & \varepsilon \leqslant \sigma_y/E \\ \sigma_y + 1929.06 + 223.90\mathrm{e}^{-\frac{(t/d-10.08)^2}{4.4402}}(\varepsilon - \sigma_y/E) & \varepsilon > \sigma_y/E \end{cases} \tag{10}$$

where E=871.11 GPa; σ_y is shown in Eq. (7); t is sheet thickness and also an internal parameter that describes the behavior of the material in relation to the thickness. The

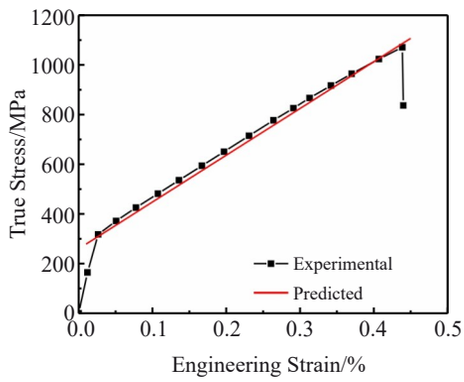

Fig. 6 Comparison of experimental and predicted results of CoCrNi MEA ultrathin strips with t/d=9.6

plastic stiffness is increased firstly and then decreased with the increase in t/d value, and it reaches a peak value when t/d value is approximately 10.

Fig.6 presents a comparison between experimental data and predicted results of CoCrNi MEA ultrathin strips when the t/d value is 9.6. It can be seen that the prediction has high accuracy.

5 Conclusions

1) The CoCrNi MEA ultrathin strips have a more pronounced size effect during the uniaxial tensile test. The reduction in the strength is mainly attributed to the surface layer effect. The t/d value is the main reference variable.

2) The uniform constitutive model equations of the elastic deformation and plastic deformation stages are constructed. The relationship between YS and t/d can be efficiently simulated using the modified formula. In the case of $6.75<t/d<10.62$, the size effect should be appropriately considered; YS and UTS are reduced with the decrease in t/d value. When the t/d value is greater than 10.62, the size effect causes the decline of YS and UTS.

3) During the plastic deformation stage, the plastic stiffness of the material is correlated with the t/d value. Initially, as the t/d value increases, the work-hardening capability is enhanced. The work-hardening capacity reaches the maximum state when the t/d value is approximately 10. When the t/d value exceeds 10, the work-hardening capacity weakens.

References

1 Vollertsen F, Hu Z, Niehoff H S *et al*. *Journal of Materials Processing Technology*[J], 2004, 151(1–3): 70

2 Gau J T, Principe C, Wang J. *Journal of Materials Processing Technology*[J], 2007, 184(1–3): 42

3 Chan W L, Fu M W. *Materials Science and Engineering A*[J], 2011, 528(25–26): 7674

4 Geiger M, Vollertsen F, Kals R. *CIRP Annals*[J], 1996, 45(1): 277

5 Kals T A, Eckstein R. *Journal of Materials Processing Technology*[J], 2000, 103(1): 95

6 Michel J F, Picart P. *Journal of Materials Processing Technology*[J], 2003, 141(3): 439

7 Wang S, Feng S K, Chen C *et al*. *International Journal of Refractory Metals and Hard Materials*[J], 2019, 80: 161

8 Sahu J, Chakrabarty S, Raghavan R *et al*. *The Journal of Strain Analysis for Engineering Design*[J], 2018, 53(7): 517

9 Yuan Z P, Tu Y Y, Yuan T *et al*. *Journal of Alloys and Compounds*[J], 2021, 859: 157752

10 Zhu C X, Xu J, Yu H P *et al*. *Journal of Materials Research and Technology*[J], 2021, 11: 2146

11 Li Wei, Yu Hui, Li Songsong *et al*. *Rare Metal Materials and Engineering*[J], 2023, 52(9): 3213 (in Chinese)

12 Song Meng, Liu Xianghua, Sun Xiangkun *et al*. *Transaction of Materials and Heat Treatment*[J], 2016, 37(S1): 5 (in Chinese)

13 Lu L, Sui M L, Lu K. *Adv Eng Mater*[J], 2001, 3(9): 663

14 Lu L, Sui M L, Lu K. *Acta Materialia*[J], 2001, 49(19): 4127

15 Chen S D, Liu X H, Liu L Z. *Transactions of Nonferrous Metals Society of China*[J], 2015, 25(10): 3370

16 Chen Shoudong, Liu Xianghua, Liu Lizhong *et al*. *Journal of Northeastern University* (*Natural Science*) [J], 2016, 37(5): 647 (in Chinese)

17 Chen Jinliang, Feng Zhongxue, Yi Jianhong. *Rare Metal Materials and Engineering*[J], 2023, 52(6): 2182 (in Chinese)

18 Shu Xiaoyong, Qiu Panpan, Hu Linli *et al*. *Rare Metal Materials and Engineering*[J], 2023, 52(2): 551 (in Chinese)

19 Wu Z, Bei H, Otto F *et al*. *Intermetallics*[J], 2014, 46: 131

20 Zhao Y L, Yang T, Tong Y *et al*. *Acta Materialia*[J], 2017, 138: 72

21 Gludovatz B, Hohenwarter A, Thurston K V S *et al*. *Nat Commun*[J], 2016, 7(1): 10602

22 Deng H W, Xie Z M, Zhao B L *et al*. *Materials Science and Engineering A*[J], 2019, 744: 241

23 Wang Huaikun, Wang Qiang, Wang Zidi *et al*. *Rare Metal Materials and Engineering*[J], 2023, 52(5): 1885 (in Chinese)

24 Hansen N. *Acta Metallurgica*[J], 1977, 25(8): 863

25 Engel U. *Wear*[J], 2006, 260(3): 265

26 Song Meng. *Rolling Experiment of Ultra-Thin Metal Strip and Its Size Effect*[D]. Shenyang: Northeastern University, 2018 (in Chinese)

27 Peng L F, Liu F, Ni J *et al*. *Materials & Design*[J], 2007, 28(5): 1731

28 Hou J X, Zhang M, Yang H J *et al*. *Metals*[J], 2017, 7(4): 111

29 Hall E O. *Proc Phys Soc B*[J], 1951, 64(9): 747

30 Petch N J. *J Iron Steel Inst*[J], 1953, 174: 25

31 Braunovic M. *Canadian Metallurgical Quarterly*[J], 1974, 13(1): 211

32 Yu D Y W, Spaepen F. *Journal of Applied Physics*[J], 2004, 95(6): 2991

33 Venkatraman R, Bravman J C. *J Mater Res*[J], 1992, 7(8): 2040

34 Messner A, Engel U, Kals R *et al*. *Journal of Materials Processing Technology*[J], 1994, 45(1–4): 371

CoCrNi中熵合金极薄带流动应力的尺寸效应

智　惠[1,2,3,4]，侯晋雄[1,2]，马胜国[1,3]，王　涛[1,2]，王志华[1,3]，黄庆学[1,2]

(1. 太原理工大学 机械工程学院，山西 太原 030024)

(2. 太原理工大学 先进金属复合材料成形技术与装备教育部工程研究中心，山西 太原 030024)

(3. 太原理工大学 航空航天学院 应用力学研究所，山西 太原 030024)

(4. 晋中学院 机械系，山西 晋中 030619)

摘　要：构建了一个考虑尺寸效应的本构模型，以分析CoCrNi中熵合金极薄带在单轴准静态拉伸试验中不同变形阶段的行为。结果表明，由于尺寸效应，传统宏观成形技术在微成形过程中的适用性受限，这一点与极薄带成形过程中厚度与直径比（*t*/*d*）的关系密切相关。在*t*/*d*低于10.62的情况下，CoCrNi合金带材在弹性变形阶段展现出明显的尺寸依赖性。随着*t*/*d*的降低，表面层晶粒的体积分数上升，导致流动应力呈线性下降趋势。在塑性变形阶段，材料的刚度与*t*/*d*呈现相关性。具体来说，随着*t*/*d*的提升，材料的加工硬化能力增强，当*t*/*d*接近10时达到峰值，超过该值后加工硬化能力开始减弱。

关键词：中熵合金；极薄带；尺寸效应；流动应力；塑性刚度

作者简介：智　惠，女，1989年生，博士，讲师，太原理工大学机械工程学院，山西 太原 030024，E-mail：zhihui0005@link.tyut.edu.com